

Article

# Long-Term Biogas Slurry Application Drives Two-Phase Succession in Sugarcane Field Soil Ecosystems: From Microbial Community Disturbance to Functional Restructuring

Jiping Wang <sup>†</sup>, Tiedong Lu <sup>†</sup> , Ye Zhang, Qin Li, Lirong Su, Zhuang Li, Tianming Su <sup>\*</sup> and Tiegua He <sup>\*</sup>

Agricultural Resources and Environment Research Institute, Guangxi Academy of Agricultural Sciences / Guangxi Key Laboratory of Arable Land Conservation, Nanning 530007, China; jpwang0110@163.com (J.W.); lutiedong@163.com (T.L.); zhangye@gxaas.net (Y.Z.); lixuanqin@126.com (Q.L.); lirongsu126@126.com (L.S.); lizhuang@gxaas.net (Z.L.)

<sup>\*</sup> Correspondence: sutianming04@126.com (T.S.); tghe118@163.com (T.H.)

<sup>†</sup> These authors contributed equally to this work.

## Abstract

Promoting the agricultural recycling of biogas slurry (BS) is crucial for sustainable development, yet its long-term ecological impacts remain unclear. Through a multi-year field trial in a sugarcane system, this study examined the effects of BS application (0, 3, and 6 years) on the soil properties, bacterial communities, and functional genes for C, N, P, and S cycling. The results revealed distinct two-phase patterns of changes in soil properties, microbial communities, and functional genes. Short-term (3-year) application induced a “disturbance” phase, characterized by significant acidification (pH decreased by 17.91%), a surge in nitrate-N (increased by 757.27%), and a transient decline in bacterial richness. Long-term (6-year) application drove a “functional restructuring” phase, reversing acidification and significantly increasing soil organic matter (29.05%) and total nitrogen (TN) (20.81%). Bacterial richness recovered, and community composition distinctively restructured. Functional gene analysis revealed shifts in gene abundance that transitioned from high abundance in the short term to a new balance favoring processes like N fixation. Co-occurrence network analysis indicated that this functional shift was associated with core microbial modules (e.g., Firmicutes) and changes in soil pH and SOM. This study suggests that, although short-term application causes significant adjustments, sustained and appropriate BS application can ultimately enhance soil fertility and promote a functionally reorganized state by reshaping microbial interaction networks. It presents a microbial ecological basis for the safe and sustainable use of BS in circular agriculture.

**Keywords:** biogas slurry; long-term application; soil microorganisms; functional genes; ecosystem succession



Academic Editor: Dinca Lucian

Received: 2 March 2026

Revised: 27 March 2026

Accepted: 27 March 2026

Published: 29 March 2026

**Copyright:** © 2026 by the authors.

Licensee MDPI, Basel, Switzerland.

This article is an open access article distributed under the terms and

conditions of the [Creative Commons Attribution \(CC BY\) license](https://creativecommons.org/licenses/by/4.0/).

## 1. Introduction

Modern intensive agriculture meets global food demand but disrupts natural cycles, leading to the separation of crop and livestock systems [1]. This separation causes environmental problems [2]. Crop production now heavily relies on chemical fertilizers, which consume energy and cause pollution [3]. Meanwhile, large livestock farms produce vast amounts of manure, which pollutes the environment and releases greenhouse gases [4,5].

To address these issues, there is a global push for a greener agricultural model [6,7]. This model aims to reconnect crop and livestock farming into a circular system, where

waste becomes a resource [8]. Biogas slurry (BS), a liquid by-product from the anaerobic digestion of livestock manure and crop residues, is important for this system [9,10]. Rich in nitrogen (N), phosphorus (P), and organic matter, BS can improve soil fertility, boost crop yields, and partially replace chemical fertilizers [11], offering a new way to recycle agricultural waste.

The benefits of using BS on farmland are well-known. Many studies show that it elevates soil organic matter (SOM) and available nutrients, enhances soil structure, and triggers crop growth [12,13]. However, BS has special properties: it contains large amounts of water and inorganic N but has a low C/N ratio. If not managed properly, applying BS can increase the emissions of strong greenhouse gases like nitrous oxide (N<sub>2</sub>O) by accelerating soil nitrification and denitrification [14,15]. Its increased water content and decreased C/N ratio also lead to unique interactions with soil, which may affect carbon (C) and N cycles differently than other fertilizers [16]. In particular, we do not fully understand how BS changes the soil microbiome—the community of microorganisms that drives all nutrient cycling—in the long term.

Most current research focuses on the short-term effects of BS, such as on crop yield or basic soil chemistry [17]. There is a lack of systematic evidence on how long-term use alters the structure and function of the soil ecosystem. In this study, we aimed to: (1) characterize the temporal dynamics of soil properties and microbial communities under long-term BS application; (2) quantify the changes in the abundance of key functional genes involved in nutrient cycling; and (3) explore the potential mechanisms linking shifts in microbial communities to functional restructuring. Specifically, we sought to understand how long-term BS application reshapes soil's bacterial communities and how these microbial changes mediate the transformation of key nutrients like C, N, and P. Understanding these mechanisms is essential for developing sustainable circular agriculture [18].

## 2. Materials and Methods

### 2.1. Study Area

The experimental location of this study was at a farm in Nanning City, Guangxi Zhuang Autonomous Region, China (22°50' N, 107°58' E). The annual mean temperature and precipitation in this region were 22° and 1194 mm, respectively. The average soil nutrients in the sugarcane area of the experiment site were as follows: the average pH was 5.19, SOM was 21.34 g/kg, total nitrogen (TN) was 1.12 g/kg, available phosphorus (AP) was 18.75 mg/kg, and available potassium (AK) was 142.46 mg/kg.

The farming system employed at the study site combined planting with breeding practices. A large area of sugarcane was cultivated around a pig farm to utilize the waste generated from breeding activities. After collection, the manure underwent filtration and sedimentation before its supernatant was transferred to an anaerobic tank for rapid anaerobic fermentation. Solids and sediments were removed from the process as compost material. The BS was delivered to the sugarcane fields via an irrigation pipeline system. The application rate of the BS was 4.5 to 6 tons per hectare, applied approximately every 20 days, with the amount and timing of application adjusted based on local weather. The slurry properties in the experiment included a pH of 7.83, TN of 0.44 g/L, total phosphorus (TP) of 13.84 mg/L, and total potassium (TK) of 0.85 g/L.

### 2.2. Soil Sampling

The collection of soil samples was conducted on 25 February 2023, after the sugarcane harvest. The experiment was conducted with three independent field plots (replicates) per treatment. Within each plot (over 0.33 hectares), top-layer soil samples (0–20 cm) were collected from 5 random points and pooled to form a single composite sample. The soil

samples were immediately transported to the lab, placed in sealed sterile plastic bags, and then filtered through a 2 mm mesh to eliminate roots and plant-derived material. One part of the samples was kept at  $-80\text{ }^{\circ}\text{C}$  for extracting DNA, while the other part was air-dried for soil property measurement.

Soil pH was assessed via a pH meter at a soil-to-water ratio of 2.5:1, while electrical conductivity (EC) was detected with a conductivity meter at a soil-to-water ratio of 1:5. TN was quantified via the Kjeldahl technique post-extraction with 2 M KCl.  $\text{NH}_4^+\text{-N}$  and  $\text{NO}_3^-\text{-N}$  were isolated with 2 M KCl and determined by colorimetric analysis. TP was measured via the molybdenum blue colorimetric technique after digestion with 5 M  $\text{H}_2\text{SO}_4$ , and AP was determined using the same method following extraction with 0.5 M  $\text{NaHCO}_3$ . TK and AK were quantified by flame photometry. SOM content was determined via the potassium dichromate volumetric technique.

### 2.3. DNA Isolation and 16S rRNA Sequencing

Total genomic DNA was isolated from 0.5 g of soil using a FastDNA Spin Kit for Soil (MP Biomedicals, Santa Ana, CA, USA) as per the manufacturer's guidelines. DNA quality, concentration, and purity were assessed by agarose gel electrophoresis and ultraviolet absorbance with a Nanodrop One spectrophotometer (Thermo Fisher Scientific, Waltham, MA, USA). The DNA level was further quantified with a QuantiFluor dsDNA kit (Promega, Madison, WI, USA). The extracted DNA was diluted to  $50\text{ ng }\mu\text{L}^{-1}$  with sterile water and kept at  $-20\text{ }^{\circ}\text{C}$  until further analysis.

Primer pairs—barcode-338F/806 R ( $5'\text{-ACTCCTACGGGAGGCAGCA-3'}/5'\text{-GGACTACHVGGGTWTCTAAT-3'}$ )—were utilized for the amplification of the V3–V4 region of the bacterial 16 S rRNA gene. To distinguish bacterial communities, the V3–V4 region of the 16S rRNA gene underwent amplifying, purifying, quantifying, pooling, and sequencing on an Illumina Nova6000 platform (Illumina, San Diego, CA, USA) at Magigene Technology Co., Ltd. (Guangzhou, China).

Each 50  $\mu\text{L}$  PCR reaction comprised 25  $\mu\text{L}$  of  $2\times$  Premix Ex Taq (Takara Biotechnology, Shiga, Japan), 1  $\mu\text{L}$  of each primer (10  $\mu\text{M}$ ), 1  $\mu\text{L}$  of template DNA (50 ng), and 21  $\mu\text{L}$  of nuclease-free water. Thermal cycling was conducted with a primary denaturation at  $94\text{ }^{\circ}\text{C}$  for 3 min, followed by 30 cycles of 30 s denaturation at  $94\text{ }^{\circ}\text{C}$ , 30 s annealing at  $58\text{ }^{\circ}\text{C}$ , and 30 s extension at  $72\text{ }^{\circ}\text{C}$ , with a final 10 min extension at  $72\text{ }^{\circ}\text{C}$ .

The raw paired-end reads were merged subsequent to adaptor trimming and removal of low-quality reads, ambiguous bases, and barcodes to produce clean sequences. Processing the high-quality sequences was conducted via Quantitative Insights Into Microbial Ecology (QIIME). Open-reference OTUs were defined at 97% sequence similarity using UPARSE, and bacterial annotation was performed against the silva\_rdp/v132\_v11.5 database.

### 2.4. HT-qPCR

Quantitative microbial element cycling (QMEC) comprised 72 primer pairs (Table S1) targeting genes involved in major C, N, P, and S biogeochemical cycling (71 primer sets) and the 16S rRNA gene [19]. HT-qPCR was conducted using a Wafergen SmartChip Real-time PCR system (WaferGen, Fremont, CA, USA) as per the manufacturer's guidelines. The amplification program comprised an initial denaturation at  $95\text{ }^{\circ}\text{C}$  for 10 min, and then 40 cycles of  $95\text{ }^{\circ}\text{C}$  for 30 s,  $58\text{ }^{\circ}\text{C}$  for 30 s, and  $72\text{ }^{\circ}\text{C}$  for 30 s. Melting curves were automatically produced by SmartChip software (WaferGen, Fremont, CA, USA).

All reactions were conducted in technical triplicates. We excluded amplifications with several melting peaks or efficiencies  $< 80\%$  or  $> 120\%$ . Only results with threshold cycle (CT) values  $< 31$  were used for subsequent analyses. Relative abundance (RA)

was measured as the ratio of functional gene abundance to 16S rRNA gene abundance (Equation (1)), while absolute gene abundance was determined depending on absolute 16S rRNA gene copy numbers quantified by conventional qPCR (Equation (2)), where Fun and 16S represent functional and 16S rRNA genes, respectively. The absolute quantitative information of 16S rRNA gene was obtained by quantitative PCR (Roche, LightCycler480II, Basel, Switzerland)

$$\text{Gene relative copy number GR} = (31 - \text{CT}) / (10/3), \quad (1)$$

$$\text{Gene absolute copy number GAFun} = \frac{\text{GA}_{16\text{s}} \cdot \text{GR}_{\text{Fun}}}{\text{GR}_{16\text{s}}}. \quad (2)$$

### 2.5. Data Analysis

Usearch-alpha\_div (v10, <http://www.drive5.com/usearch/>, accessed on 10 May 2024) and R were utilized to assess the bacterial richness, diversity, and evenness indices (Chao1, richness, abundance-based coverage estimator (ACE), Shannon, and Simpson). One-way analyses of variance (ANOVA) was utilized to assess significant variations among treatments via SPSS 25.0 (IBM Corp, Armonk, NY, USA). R software's vegan package (v 2.6) was applied to perform principal coordinates analysis (PCoA). The bar chart was created using Origin 2018, and the heatmap was established via R pheatmap (v1.0.12). The correlation network was plotted with Gephi (version 0.10.1). Other data organization and analyses were conducted using Microsoft Excel 2019.

## 3. Results

### 3.1. Effects of Adding BS on Soil Properties

The addition of BS to soil significantly altered the physicochemical properties of the soil matrix. Comparative analysis revealed that the treatments with added BS, namely BS3 and BS6, exhibit pronounced differences in pH, AP, AK,  $\text{NO}_3^-$ -N, and  $\text{NH}_4^+$ -N when compared to BS0. Notably, the BS6 treatment showed a significant increase in SOM content (Table 1).

**Table 1.** Characteristics of physicochemical properties of BS and soil.

Treatments	pH	TN (g kg <sup>-1</sup> )	TP (g kg <sup>-1</sup> )	TK (g kg <sup>-1</sup> )	EC (ms cm <sup>-1</sup> )	AP (mg kg <sup>-1</sup> )	AK (mg kg <sup>-1</sup> )	$\text{NO}_3^-$ -N (mg kg <sup>-1</sup> )	$\text{NH}_4^+$ -N (mg kg <sup>-1</sup> )	SOM (g kg <sup>-1</sup> )
BS0	5.92 ± 0.30 a	1.56 ± 0.04 b	1.37 ± 0.12 a	0.38 ± 0.16 a	0.14 ± 0.02 a	321.98 ± 17.33 a	573.52 ± 41.03 a	6.74 ± 0.22 b	2.36 ± 0.19 c	26.77 ± 1.30 b
BS3	4.86 ± 0.27 b	1.5 ± 0.06 b	0.69 ± 0.26 b	0.34 ± 0.04 a	0.2 ± 0.04 a	59.28 ± 8.42 c	547.45 ± 25.51 a	57.78 ± 8.90 a	3.46 ± 0.09 a	24.43 ± 1.52 b
BS6	6.36 ± 0.22 a	1.97 ± 0.07 a	0.75 ± 0.16 b	0.26 ± 0.02 a	0.13 ± 0.02 a	207.07 ± 13.21 b	267.61 ± 17.53 b	4.54 ± 1.30 b	3.03 ± 0.06 b	37.73 ± 1.58 a

Values in the table are the mean ± SE; different letters in the same column indicate a significant difference ( $p < 0.05$ ).

Compared to BS0, the BS3 treatment caused significant reductions in soil pH, TP, and AP by 17.91%, 49.64%, and 81.59%, respectively. In contrast,  $\text{NO}_3^-$ -N and  $\text{NH}_4^+$ -N concentrations increased dramatically by 757.27% and 46.61%. In addition, TN,  $\text{NH}_4^+$ -N, and SOM contents in BS6 were significantly higher than those in BS0 by 20.81, 22.11, and 29.05%. The contents of TP, AP and AK were significantly lower in BS6 than those in BS0.

Compared to BS3, pH, TN, and SOM contents in BS6 were significantly increased by 30.86, 31.33, and 54.44%, while  $\text{NO}_3^-$ -N and  $\text{NH}_4^+$ -N contents were significantly decreased by 92.14 and 12.43%, respectively.

### 3.2. Bacterial Diversity

#### 3.2.1. $\alpha$ Diversity

Bacterial  $\alpha$  diversity was remarkably influenced by different application durations of BS. Chao1, richness and ACE were utilized as richness indices, and the Shannon\_2 and Simpson indices were utilized as diversity indices. Significant variations were detected in the richness index of the bacterial community in sugarcane soil from BS0 to BS6 (Table 2), with a trend characterized by a primary reduction, followed by an elevation ( $p < 0.05$ ). The microbial diversity, as illustrated by both the Shannon and Simpson indices, also exhibited significant differences among the three treatments (Figure 1).

**Table 2.** Changes in the richness indices of the soil bacterial communities in the different treatments.

Treatments	Chao1	Richness
BS0	4164.27 $\pm$ 301.29 b	4163.67 $\pm$ 301.37 b
BS3	3257.77 $\pm$ 148.97 c	3257.00 $\pm$ 149.07 c
BS6	4945.53 $\pm$ 85.21 a	4945.33 $\pm$ 85.26 a

Values in the table are the mean  $\pm$  SE; different letters in the same column indicate a significant difference ( $p < 0.05$ ).

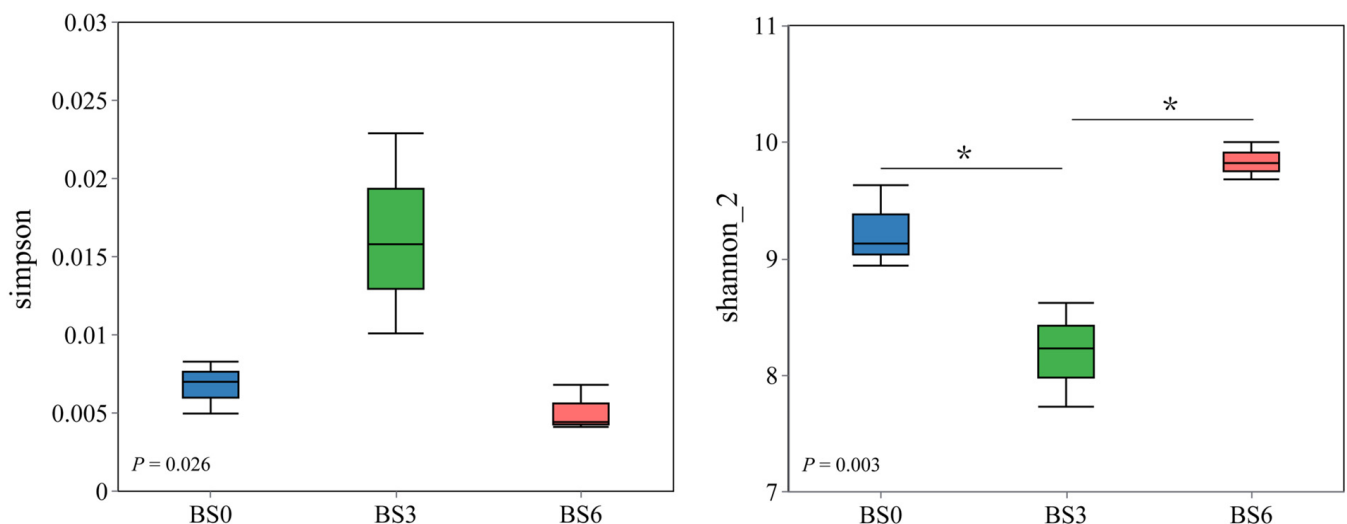


**Figure 1.** Differences in the diversity indices of soil bacterial communities across different treatments. \* indicates significant differences among treatments ( $p < 0.05$ ,  $t$ -test).

#### 3.2.2. $\beta$ Diversity

The PCoA plot clearly delineates significant variations in the composition of the bacterial microbial communities among the three groups of soil samples (Figure 2B), with the first principal coordinate (PCoA1) accounting for 46.6% of the dataset's variability. The pronounced divergence of the samples along the PCoA1 indicates that the duration of BS application had a substantial impact on soil microbial diversity. On the second principal coordinate (PCoA2), there is a significant distinction between the BS3, BS6, and BS0 groups, with BS3 and BS6 showing greater similarity to each other. This suggested that the microbial community composition of soils treated with BS differed markedly from that of untreated soils.

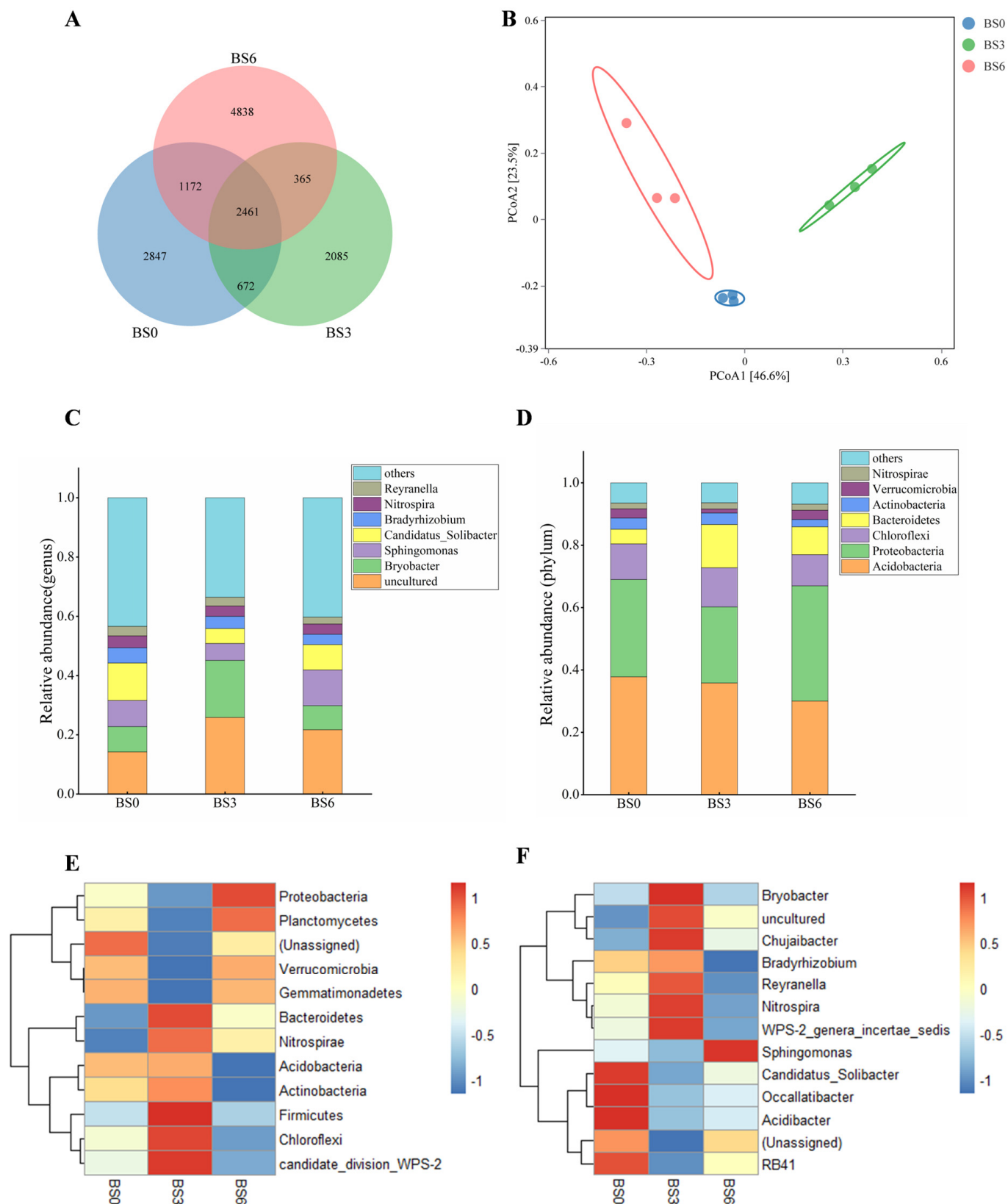


**Figure 2.** Analysis of Soil Bacterial Community Diversity. (A): OTU Venn diagram; (B): PCoA analysis; (C,D): Microbial community structure at the phylum and genus levels under different treatments. (relative abundance > 1%); (E,F): Clustering analysis of species at the phylum and genus levels. (relative abundance > 0.5%).

### 3.3. Microbial Community Structure Composition

The results of community structure analysis at the OTU level indicated that there were 2461 OTUs common to all three groups. The numbers of OTUs unique to BS0, BS3, and BS6 were 2847, 2085, and 4835, respectively (Figure 2A). Compared to BS0, the number of unique OTUs in BS6 was higher by 69.93%.

Figure 2C illustrate the RA of the key soil bacterial taxa. Acidobacteria, Proteobacteria, Chloroflexi, and Bacteroidetes were the dominant phyla in the sugarcane soil in all treatments, consisting of 85.12–86.65% of the total RA. Other phyla with high RA included Actinobacteria (2.32–3.70%), Verrucomicrobia (1.26–2.99%), and Nitrospirae (1.85–2.00%). Among these, compared to the other treatments, Proteobacteria and Verrucomicrobia in BS3 were significantly lower ( $p < 0.05$ ) by 21.79–34.07% and 57.56–57.89%. Compared to BS0, among the phyla with an RA greater than 0.5%, the RA of Bacteroidetes and Nitrospirae increased in the soil with digested BS. As the duration of digested BS application increases, the RA of Proteobacteria, Planctomycetesta, Verrucomicrobia, Gemmatimonadetes were lower in BS3 but subsequently higher in BS6. Conversely, the RA of Acidobacteria, Actinobacteria, Firmicutes, Chloroflexi, candidate\_division\_WPS-2 exhibited an opposite trend.

At the genus level, the RA of uncultured genera in BS3 and BS6 was higher than that in BS0 (Figure 2D). The predominant soil bacterial taxa included *Bryobacter* (8.14–19.23%), *Sphingomonas* (5.72–12.09%), *Candidatus\_Solibacter* (5.02–12.62%), *Bradyrhizobium* (3.48–5.14%), *Nitrospira* (3.34–4.03%), *Reyranella* (2.95–3.20%). The RA of *Bryobacter*, *uncultured*, *Chujaibacter*, *Bradyrhizobium*, *Reyranella*, *Nitrospira*, and *WPS-2\_genera\_incertae\_sedis* was higher in BS3 but lower in BS6 as the period of digested BS application increased. On the other hand, there was an opposite trend in the RA of *Sphingomonas*, *Candidatus\_Solibacter*, *Occallatibacter*, *Acidibacter*, and *RB41*.

### 3.4. Quantitative Analysis of C, N, P, and S Biogeochemical Cycling

Quantitative analysis of 71 C-, N-, P-, and S-metabolism-related genes (Table S1) was conducted on all samples. A total of 61 genes were detected, accounting for 85.92% of the total. Among them, 52 genes were detected in all treatments, with two unique genes each for BS3 and BS6. All functional genes present in BS0 were also present in BS3 (Figure 3A).

The absolute abundance of genes was statistically analyzed for each class (Figure 3B). Among all treatments, BS3 exhibited the highest total functional gene abundance for each class, while BS6 had the lowest. Genes of N cycling, C fixation, and C degradation were the main classes in the soil. Specifically, for genes correlated with C cycling, including C fixation and methane metabolism, BS3 showed a significantly higher total abundance compared to BS0 and BS6. Additionally, the absolute abundance of P cycling genes was significantly higher in BS3 compared to BS6.

Among the top 30 most abundant functional genes (Figure 3C), *nifS2*, *nirS1*, and *nifH* were found to have the highest content in BS6, with all three genes participating in N cycling. Nineteen functional genes were more abundant in BS3, and their abundance exhibited a trend of elevating initially and then declining over time as the BS application proceeded. This group of genes included five N cycling genes (*nirK3*, *nosZ1*, *nxrA*, *nosZ2*, and *amoA1*), six C fixation genes (*frdA*, *accA*, *mct*, *acsA*, *smtA*, *pccA*), three C degradation genes (*xylA*, *manB*, *sga*), three P cycling genes (*ppx*, *gcd*, *phnK*), one methane metabolism gene (*pmoA*), and one sulfur cycling gene (*apsA*).

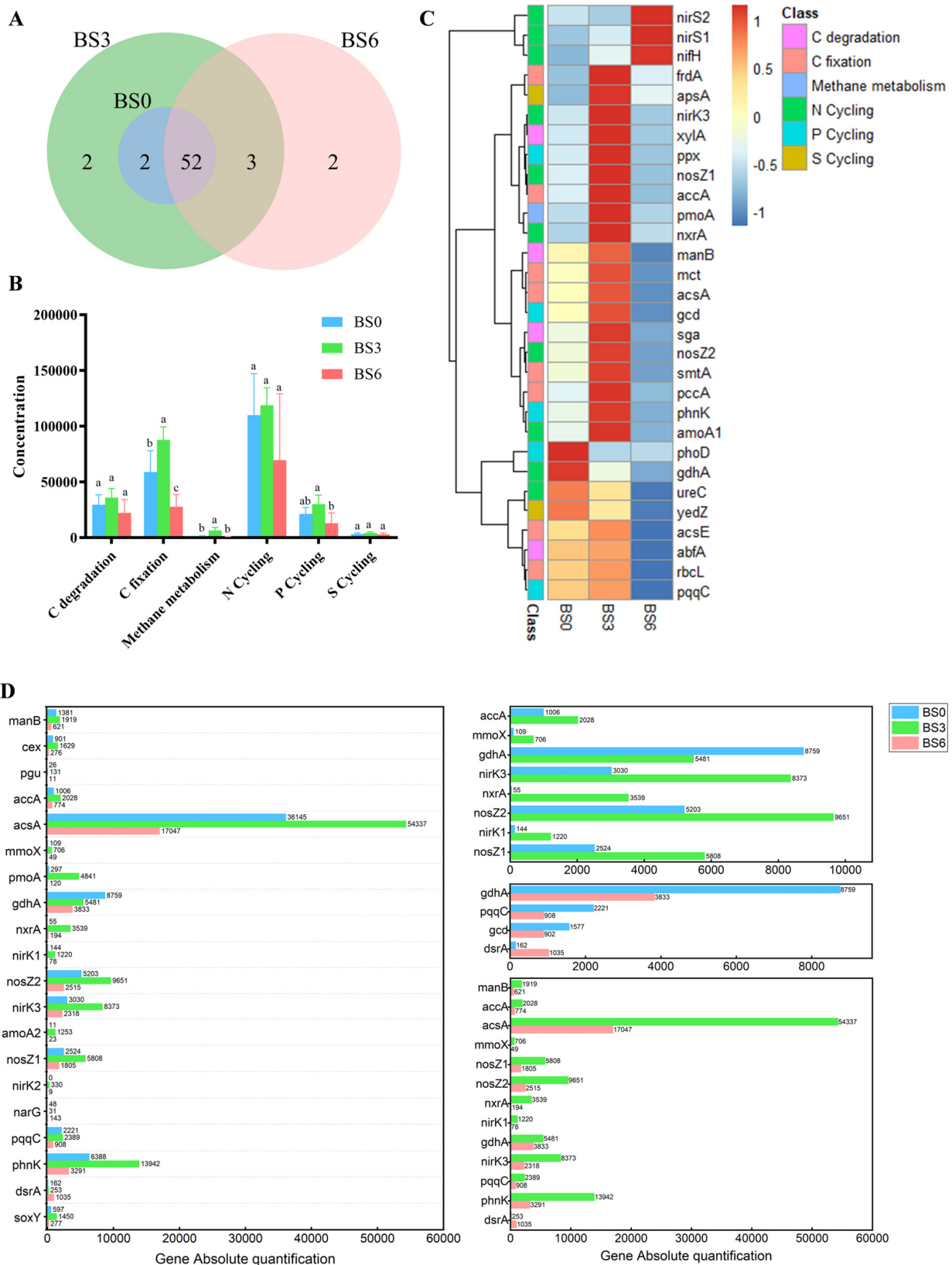


**Figure 3.** Quantitative Analysis of Soil Functional Genes. (A): Venn diagram of the number of soil functional genes detected under different treatments; (B): Concentration of CNPS functional genes under different treatments. Different letters indicate significant differences among treatments ( $p < 0.05$ , one-way ANOVA); (C): Clustering analysis heatmap of the top 30 functional genes ranked by absolute abundance; (D): Results of significant differences in functional gene abundance among different treatments ( $p < 0.05$ ).

### 3.5. Differential Analysis of Functional Genes

In the quantitative comparisons of the functional genes across the three treatments, the results illustrated that there were 20 genes showing significant variations among the groups (Figure 3D). A total of 45.00% of the differentially expressed functional genes were related to N cycling, which accounted for the highest proportion. A total of 17 of the 20 functional genes absolute abundance tended to rise initially and then decrease with the extension of the BS application period. *ghdA* showed a declining trend, and *narG* and *dsrA* exhibited an increasing trend, despite their relatively lower absolute abundance.

Compared BS3 to BS0, there were significant differences in eight genes. Among them, six genes (*ghdA*, *nirK3*, *nxrA*, *nosZ2*, *nirK1*, *nosZ*) are related to N cycling, and two genes (*accA*, *mmoX*) are related to C cycling. Except *ghdA*, the abundances of other differential genes were significantly higher in BS3 than in BS0. In the comparison between BS0 and BS6, there were four functional genes with significant differences in abundance. Except for *dsrA*, which had a significantly elevated absolute abundance in BS6 compared to BS0, the other three genes were significantly more abundant in BS0. Twelve genes showed significantly higher absolute abundances in BS3 compared to BS6, encompassing four C cycle genes (*manB*, *accA*, *acsA*, *mmoX*), six N cycle genes (*nosZ1*, *nosZ2*, *nxrA*, *nirK1*, *ghdA*, *nirK3*), and two P cycle genes (*pqqC*, *phnK*). *dsrA* was the only exception, with its abundance significantly higher in BS6 than in BS3.

## 4. Discussion

### 4.1. Long-Term Application of BS Changed Soil Physicochemical Properties

BS is rich in nutrients, and its application has shown significant agronomic benefits [20]. In the present study, compared to BS0, soil of BS3 exhibited a significant decrease in pH, a significant reduction in AP and TP, while nitrate nitrogen ( $\text{NO}_3^-$ -N) content increased markedly by 7.6-fold (Table 1). We hypothesize that BS application supplies both water and nutrients, thereby promoting crop production and leading to the depletion of specific soil nutrients such as P [21]. Meanwhile, the nutrient input from BS itself had a relatively low P content (TP of 13.84 mg/L), which may have been insufficient to offset P removal from the system. In the absence of crop yield or nutrient balance data, this proposed mechanism requires further validation. Concurrently, the input of BS alters the soil functional gene abundance, suggesting an enhanced genetic potential for nitrification as indicated by a substantial 64-fold increase in the abundance of the *nxrA* gene (Figure 3D). This elevated nitrification potential may contribute to the generation of  $\text{NO}_3^-$ -N and  $\text{H}^+$  ions, which is consistent with the observed soil acidification in the early stage of BS application [12]. The BS6 exhibited an elevation in pH and TN content compared to the BS0 and BS3. With the progression of time since the application of BS, there is a discernible cumulative effect on soil pH, resulting in an elevation of the soil's pH level [22]. The SOM content in sugarcane fields has exhibited a significant increase after six years of adding BS, corroborating previous studies [22,23]. Organic matter, which is recalcitrant to direct utilization as a soil nutrient [24], has been observed to accumulate progressively with sustained application. In addition to indicators such as pH and organic matter that are susceptible to cumulative effects, nutrient indices N, P, and K have shown fluctuations after three years of BS application and gradually approached the levels of the control group after six years. We hypothesize that an autoregulatory effect between soil and crops balances nutrient content in the soil through the growth of sugarcane [25].

#### 4.2. Effects of BS Treatment on Bacterial Diversity and Communities

The integrity of soil microbial communities is essential for the optimal functioning of agricultural ecosystems. Soil bacterial populations exhibit pronounced sensitivity to modifications in soil characteristics that are precipitated by the application of fertilizers. Long-term application of BS alters soil microbial richness. As an anaerobic digestion product, BS typically contains abundant microbial populations including Firmicutes, Bacteroidetes, and Proteobacteria, among other microorganisms (Figure 2C,E). Its prolonged application is likely to alter the original soil microbial community structure [26]. Among the dominant soil microbial populations, the BS6 treatment increased soil pH, leading to a decline in acidophilic Acidobacteria. Meanwhile, the continuous input of Proteobacteria-rich BS resulted in increased RA of these two microbial groups in soil.

At the genus level, the RA of *Bryobacter*—a beneficial genus involved in organic matter decomposition—increased, particularly under short-term slurry application (3 years). Compared to the control, the soil subjected to 3 years of BS application showed a significantly lower in the Shannon index (Figure 1). In contrast, this index demonstrated a significant increase in BS6 compared to BS3, while it did not differ significantly between BS6 and the control. We speculate that this phenomenon could be attributed to the elevated SOM content introduced by BS, which altered the original soil environment, with more pronounced effects during the initial stage [27]. Concurrently, microorganisms associated with BS were directly introduced into the soil. The combined effects of these factors led to a rapid increase in *Bryobacter* in the BS3 treatment (Figure 2D,F), which outcompeted other less-adaptable microbial taxa, resulting in a decline in the microbial diversity indices [28]. As the application period extended, the self-regulatory capacity of the soil environment became evident, leading to an elevation in microbial diversity and a recovery of the Shannon index to pre-application levels. This suggested that the sugarcane field exhibited good tolerance to BS application and that sustained moderate application had minimal impacts on soil bacterial diversity [29].

The correlation analysis revealed that the  $\alpha$ -diversity indices were significantly positively correlated with pH and SOM, while showing significant negative correlations with AK and  $\text{NO}_3^-$ -N (Table 3). pH might be the key soil parameter that influences microbial components, diversity, and biomass in soil [30]. Soil microorganisms serve as the primary drivers of soil C and N decomposition [31], and higher SOM can stimulate the growth and diversity of soil microorganisms [32]. For acidic sugarcane field soil, the application of BS may influence soil microbial richness by altering key parameters such as soil pH and SOM.

**Table 3.** Correlations between soil properties and microbial richness and diversity indices.

Item	Richness	ACE
pH	0.87 **	0.82 **
TN	0.67 *	0.65
TP	0.03	−0.02
TK	−0.52	−0.54
EC	−0.62	−0.57
AP	0.53	0.50
AK	−0.73 *	−0.77 *
$\text{NO}_3^-$ -N	−0.883 **	−0.850 **
$\text{NH}_4^+$ -N	−0.48	−0.52
SOM	0.77 *	0.73 *

\*\* Significant at the 0.01 level ( $p < 0.01$ ); \* significant at the 0.05 level ( $p < 0.05$ ).

### 4.3. Effects of BS Treatment on CNPS Functional Genes Abundances

This study investigated the abundance of C, N, P, and S (CNPS) cycling genes in sugarcane field soils under long-term BS application. The results revealed a broad diversity of functional genes participating in main biogeochemical processes (e.g., C degradation, methane metabolism, nitrification, P solubilization, and sulfur oxidation), underscoring their essential roles in soil nutrient cycling and crop growth. Notably, the composition of CNPS cycling genes varied significantly with the duration of slurry application, a pattern likely associated with alterations in microbial community structure and the direct input of nutrients from the slurry.

To elucidate the potential associations between CNPS cycling genes and bacterial taxa, we constructed a co-occurrence network based on Spearman’s rank correlation analysis ( $r > 0.6, p < 0.05$ ) at the phylum and genus levels (Figure 4, Table S2). At the phylum level, the network included 53 nodes and 139 edges, representing 16 bacterial phyla and 37 CNPS cycling genes (Figure 4A). Firmicutes emerged as a key taxon, significantly correlated with 21 functional genes. It showed strong positive correlations with 10 C cycle genes (e.g., *cex*, *acsA*, *pmoA*), which is consistent with its reported role in decomposing complex organic matter and facilitating C transformation [33]. In the N cycle, Firmicutes positively correlated with denitrification genes (*nosZ*, *nirK*) and ammonia oxidation genes (*amoA*) but negatively correlated with *narG*, which is involved in nitrate reduction. Moreover, the relative abundance of Firmicutes (Figure 2C) showed a trend consistent with the abundance changes in the *nosZ* and *nirK* genes, further supporting the potential role of this phylum in denitrification processes. These statistical associations suggest a role for Firmicutes in denitrification, which aligns with previous reports [34].

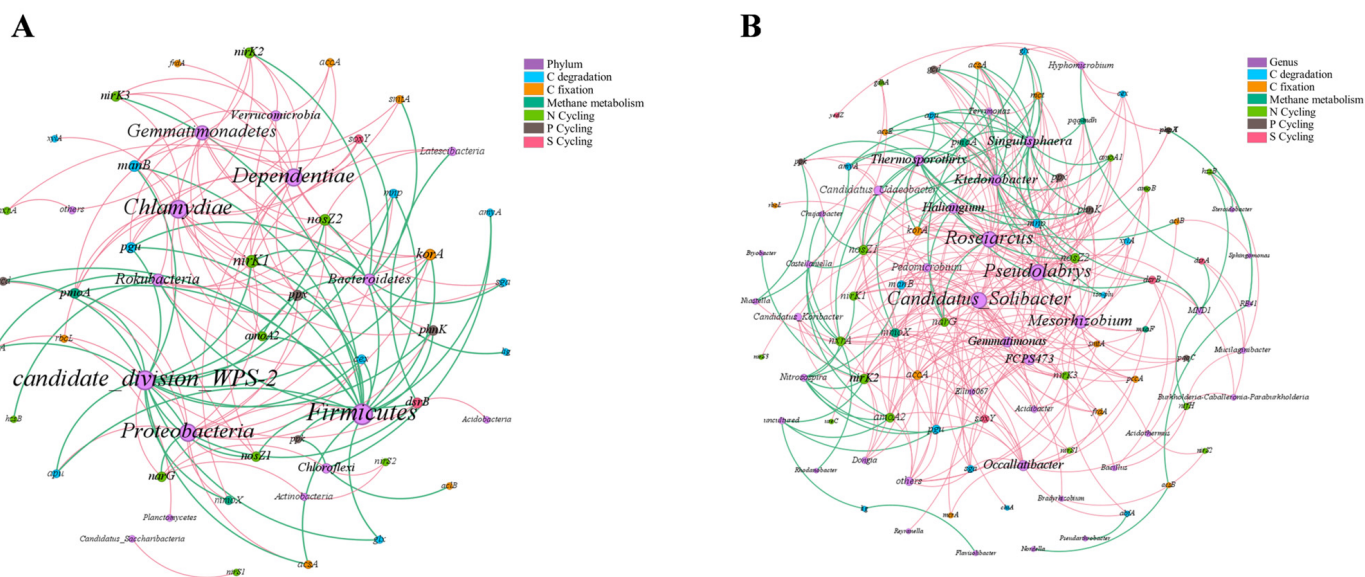


**Figure 4.** Correlation network between bacterial communities (relative abundance > 0.1%) and functional gene abundances: (A) phylum level; (B) genus level. Red and green edges indicate negative and positive correlations, respectively.

Similarly, the candidate division WPS-2 significantly correlated with 19 functional genes, including six involved in C degradation (e.g., *cex*, *pgu*), suggesting its metabolic versatility. Notably, the relative abundance of candidate division WPS-2 (Figure 2E) exhibited a trend consistent with the abundance changes in the *pgu* gene (Figure 3D), which was enriched in BS3 and declined in BS6. Originally identified in Antarctic soils, WPS-2 has been proposed to perform “atmospheric chemosynthesis” [35], and its members are known to degrade complex polysaccharides. Conversely, the parasitic phyla Chlamydiae

and Dependitiae significantly negatively correlated with multiple functional genes. This may be associated with their obligate parasitic lifestyle: a decline in their RA likely reduces the metabolic burden on host bacteria [36,37], thereby potentially contributing to a more active and diverse bacterial community, which may in turn be associated with an increase in functional gene abundance.

At the genus level, the network was more complicated, comprising 97 nodes and 347 edges, including 40 bacterial genera and 57 CNPS cycling genes (Figure 4B, Table S3). Several genera—*Nitrosospira*, *Thermosporothrix*, *Singulisphaera*, and *Ktedonobacter*—were identified as key functional hubs. They showed significant positive correlations with a suite of 21 genes spanning C (13), N (4), and P (4) cycling, which suggests their multifunctional roles in nutrient transformation. *Nitrosospira*, a known ammonia oxidizer, carries key N cycle genes such as *norB* and *nirK* [38], consistent with its positive correlations with N cycling genes in our network. Likewise, *Thermosporothrix*, *Singulisphaera*, and *Ktedonobacter* are all documented for their capability to break down organic matter, including complex compounds [39–41], supporting the strong correlations with C degradation genes observed here. It should be emphasized that these network-derived patterns represent statistical associations and are intended to generate hypotheses for future mechanistic studies rather than to serve as direct evidence of functional restructuring at the ecosystem level.

In summary, long-term BS application was associated with changes in the abundance of nutrient cycling genes in sugarcane soil, and these changes correlated with the restructuring of the microbial community. Specifically, the increased RA of organic-degrading bacteria (especially those targeting complex polymers) and anaerobic ammonia-oxidizing bacteria correlated positively with C and N cycling gene abundance. Conversely, obligate parasitic bacteria were negatively associated with functional gene abundance, a pattern that may reflect their adverse effects on host growth and metabolic activity.

## 5. Conclusions

This study demonstrates a temporal transition from short-term disturbance to long-term functional restructuring under the experimental conditions. Initial short-term (3-year) application was associated with a “disturbance” phase, characterized by nitrification-associated acidification and transient diversity loss. In contrast, prolonged (6-year) application was associated with a “functional restructuring” phase, where cumulative organic input was associated with enhanced buffering capacity and with a functionally reorganized state through microbial network reorganization. Crucially, the transformation was associated with topological evolution of the interaction network: metabolically versatile hubs showed stable correlations with C/N cycling, while the decline in parasitic groups was inversely associated with functional gene abundance. This study indicates that in sugarcane field systems, sustained and appropriate application of BS, despite inducing significant adjustments in the short term, may enhance soil fertility—particularly organic matter content—and maintain the stability of microbial diversity and key ecological functions in the long run. It represents a sustainable management strategy that synergistically promotes the resource use of agricultural waste and the improvement of soil health. The findings provide a basis for local integrated crop–livestock recycling agricultural models, pending further validation in broader contexts.

**Supplementary Materials:** The following supporting information can be downloaded at: <https://www.mdpi.com/article/10.3390/app16073319/s1>, Table S1: QMEC genes and primer pairs. Table S2: Phylum level. Table S3: Genus level.

**Author Contributions:** Conceptualization, J.W. and T.S.; methodology, J.W., Q.L. and Z.L.; formal analysis, J.W., T.L., L.S. and Z.L.; investigation, Y.Z., Q.L. and L.S.; data curation, Y.Z.; writing—original draft preparation, J.W.; writing—review and editing, J.W. and T.H.; visualization, J.W. and Q.L.; supervision, T.L. and T.S.; project administration, T.H. and T.S.; funding acquisition, J.W. and T.L. All authors have read and agreed to the published version of the manuscript.

**Funding:** This research was funded by the Natural Science Foundation of Guangxi Zhuang Autonomous Region (2023GXNSFBA026310, 2024GXNSFAA010497), the Fund of Guangxi Academy of Agricultural Science (2023JZ14, 2024YP012, 2026YT148) as well as the earmarked fund for China Agriculture Research System Guangxi Innovation Team (nycytxgxcxtd-2026-01).

**Institutional Review Board Statement:** Not applicable.

**Informed Consent Statement:** Not applicable.

**Data Availability Statement:** The raw data supporting the conclusions of this article will be made available by the authors on request.

**Conflicts of Interest:** The authors declare no conflicts of interest.

## References

1. Khatri, P.; Kumar, P.; Shakya, K.S.; Kirlas, M.C.; Tiwari, K.K. Understanding the intertwined nature of rising multiple risks in modern agriculture and food system. *Environ. Dev. Sustain.* **2024**, *26*, 24107–24150. [CrossRef]
2. Taifouris, M.; Martín, M. Integrating intensive livestock and cropping systems: Sustainable design and location. *Agric. Syst.* **2022**, *203*, 103517. [CrossRef]
3. Abebe, T.G.; Tamtam, M.R.; Abebe, A.A.; Abtemariam, K.A.; Shigut, T.G.; Dejen, Y.A.; Haile, E.G. Growing Use and Impacts of Chemical Fertilizers and Assessing Alternative Organic Fertilizer Sources in Ethiopia. *Appl. Environ. Soil Sci.* **2022**, *2022*, 4738416. [CrossRef]
4. Ijaz, M.U.; Akbar, A.; Eman, R.; Hayat, M.F.; Naz, H.; Ashraf, A. Mitigating Nutrient Pollution from Livestock Manure: Strategies for Sustainable Management. In *Agricultural Nutrient Pollution and Climate Change: Challenges and Opportunities*; Hussain, N., Hung, C., Wang, L., Eds.; Springer Nature: Cham, Switzerland, 2025; pp. 165–187.
5. Chadwick, D.; Sommer, S.; Thorman, R.; Fanguero, D.; Cardenas, L.; Amon, B.; Misselbrook, T. Manure management: Implications for greenhouse gas emissions. *Anim. Feed Sci. Tech.* **2011**, *166–167*, 514–531. [CrossRef]
6. Pe'Er, G.; Zinngrebe, Y.; Moreira, F.; Sirami, C.; Schindler, S.; Müller, R.; Bontzorlos, V.; Clough, D.; Bezák, P.; Bonn, A.; et al. A greener path for the EU Common Agricultural Policy. *Science* **2019**, *365*, 449–451. [CrossRef]
7. Sulc, R.M.; Franzluebbbers, A.J. Exploring integrated crop–livestock systems in different ecoregions of the United States. *Eur. J. Agron.* **2014**, *57*, 21–30. [CrossRef]
8. Lemaire, G.; Franzluebbbers, A.; Carvalho, P.C.D.F.; Dedieu, B. Integrated crop–livestock systems: Strategies to achieve synergy between agricultural production and environmental quality. *Agric. Ecosyst. Environ.* **2014**, *190*, 4–8. [CrossRef]
9. Jiang, Y.; Zhang, Y.; Li, H. Research Progress and Analysis on Comprehensive Utilization of Livestock and Poultry Biogas Slurry as Agricultural Resources. *Agriculture* **2023**, *13*, 2216. [CrossRef]
10. Wang, Q.; Huang, Q.; Wang, J.; Li, H.; Qin, J.; Li, X.; Gouda, S.G.; Liu, Y.; Liu, Q.; Guo, G.; et al. Ecological circular agriculture: A case study evaluating biogas slurry applied to rice in two soils. *Chemosphere* **2022**, *301*, 134628. [CrossRef]
11. Kumar, A.; Verma, L.M.; Sharma, S.; Singh, N. Overview on agricultural potentials of biogas slurry (BGS): Applications, challenges, and solutions. *Biomass Convers. Biorefin.* **2023**, *13*, 13729–13769. [CrossRef]
12. Rahaman, M.A.; Zhang, Q.; Shi, Y.; Zhan, X.; Li, G. Biogas slurry application could potentially reduce N<sub>2</sub>O emissions and increase crop yield. *Sci. Total Environ.* **2021**, *778*, 146269. [CrossRef] [PubMed]
13. Yu, F.; Luo, X.; Song, C.; Zhang, M.; Shan, S. Concentrated biogas slurry enhanced soil fertility and tomato quality. *Acta Agric. Scand. Sect. B—Soil Plant Sci.* **2010**, *60*, 262–268. [CrossRef]
14. Zou, Z.; Li, Y.; Ren, X.; Zhao, Z.; Du, Z.; Wu, D. Potential effect of biogas slurry application to mitigate of peak N<sub>2</sub>O emission without compromising crop yield in North China Plain cropping systems. *Appl. Soil Ecol.* **2025**, *210*, 106083. [CrossRef]
15. Ke, L.; Liu, X.; Du, B.; Wang, Y.; Zheng, Y.; Li, Q. Component analysis and risk assessment of biogas slurry from biogas plants. *Chin. J. Chem. Eng.* **2022**, *44*, 182–191. [CrossRef]
16. Yu, B.; Yang, K.; Zhang, Y.; Qian, X.; Li, X.; Ouyang, S.; Chen, Z. Continuous Four-Year Biogas Slurry Application Regulates the Soil Fertility, Microbial Communities, and Nitrogen Cycling Functions in a Farmland Ecosystem. *Land Degrad. Dev.* **2025**. [CrossRef]

17. Xu, M.; Xian, Y.; Wu, J.; Gu, Y.; Yang, G.; Zhang, X.; Peng, H.; Yu, X.; Xiao, Y.; Li, L. Effect of biogas slurry addition on soil properties, yields, and bacterial composition in the rice-rape rotation ecosystem over 3 years. *J. Soil. Sediment.* **2019**, *19*, 2534–2542. [[CrossRef](#)]
18. Glockow, T.; Kaster, A.; Rabe, K.S.; Niemeyer, C.M. Sustainable agriculture: Leveraging microorganisms for a circular economy. *Appl. Microbiol. Biotechnol.* **2024**, *108*, 452. [[CrossRef](#)]
19. Zheng, B.; Zhu, Y.; Sardans, J.; Peñuelas, J.; Su, J. QMEC: A tool for high-throughput quantitative assessment of microbial functional potential in C, N, P, and S biogeochemical cycling. *Sci. China Life Sci.* **2018**, *61*, 1451–1462. [[CrossRef](#)]
20. Yan, L.; Liu, Q.; Liu, C.; Liu, Y.; Zhang, M.; Zhang, Y.; Zhang, Y.; Gu, W. Effect of swine biogas slurry application on soil dissolved organic matter (DOM) content and fluorescence characteristics. *Ecotoxicol. Environ. Saf.* **2019**, *184*, 109616. [[CrossRef](#)]
21. Gupta, R.K.; Bhatt, R.; Sidhu, M.S.; Dhingra, N.; Alataway, A.; Dewidar, A.Z.; Mattar, M.A. Evaluating Biogas Slurry for Phosphorus to Wheat in a Rice–Wheat Cropping Sequence. *J. Soil Sci. Plant Nut.* **2023**, *23*, 3726–3734. [[CrossRef](#)]
22. Ren, T.; Yu, X.; Liao, J.; Du, Y.; Zhu, Y.; Jin, L.; Wang, B.; Xu, H.; Xiao, W.; Chen, H.Y.H.; et al. Application of biogas slurry rather than biochar increases soil microbial functional gene signal intensity and diversity in a poplar plantation. *Soil Biol. Biochem.* **2020**, *146*, 107825. [[CrossRef](#)]
23. Yin, G.; Wang, X.; Du, H.; Shen, S.; Liu, C.; Zhang, K.; Li, W. N<sub>2</sub>O and CO<sub>2</sub> emissions, nitrogen use efficiency under biogas slurry irrigation: A field study of two consecutive wheat-maize rotation cycles in the North China Plain. *Agric. Water Manag.* **2019**, *212*, 232–240. [[CrossRef](#)]
24. Johnston, A.E. Soil organic matter, effects on soils and crops. *Soil Use Manag.* **1986**, *2*, 97–105. [[CrossRef](#)]
25. Cheng, Y.; Zhang, J.; Cai, Z. Key Role of Matching of Crop-specific N Preference, Soil N Transformation and Climate Conditions in Soil N Nutrient Management. *Acta Pedol. Sin.* **2019**, *56*, 507–515.
26. Abubaker, J.; Cederlund, H.; Arthurson, V.; Pell, M. Bacterial community structure and microbial activity in different soils amended with biogas residues and cattle slurry. *Appl. Soil Ecol.* **2013**, *72*, 171–180. [[CrossRef](#)]
27. Herrmann, A.; Kage, H.; Taube, F.; Sieling, K. Effect of biogas digestate, animal manure and mineral fertilizer application on nitrogen flows in biogas feedstock production. *Eur. J. Agron.* **2017**, *91*, 63–73. [[CrossRef](#)]
28. Liu, Y.; Chi, Y.; Dong, Y.; Ye, B.; Fan, Z.; Nie, X.; Xing, J. Variation of nutrient content and microbial community in soils under different application years of biogas slurry. *J. Plant Nutr. Fertil.* **2023**, *29*, 483–495.
29. Meng, X.; Zeng, B.; Wang, P.; Li, J.; Cui, R.; Ren, L. Food waste anaerobic biogas slurry as fertilizer: Potential salinization on different soil layer and effect on rhizobacteria community. *Waste Manag.* **2022**, *144*, 490–501. [[CrossRef](#)]
30. Zhalnina, K.; Dias, R.; de Quadros, P.D.; Davis-Richardson, A.; Camargo, F.A.O.; Clark, I.M.; Mcgrath, S.P.; Hirsch, P.R.; Triplett, E.W. Soil pH Determines Microbial Diversity and Composition in the Park Grass Experiment. *Microb. Ecol.* **2015**, *69*, 395–406. [[CrossRef](#)]
31. Louis, B.P.; Maron, P.; Viaud, V.; Leterme, P.; Menasseri-Aubry, S. Soil C and N models that integrate microbial diversity. *Environ. Chem. Lett.* **2016**, *14*, 331–344. [[CrossRef](#)] [[PubMed](#)]
32. Zhong, W.; Gu, T.; Wang, W.; Zhang, B.; Lin, X.; Huang, Q.; Shen, W. The effects of mineral fertilizer and organic manure on soil microbial community and diversity. *Plant Soil* **2010**, *326*, 511–522. [[CrossRef](#)]
33. Huang, J.; Gao, K.; Yang, L.; Lu, Y. Successional action of Bacteroidota and Firmicutes in decomposing straw polymers in a paddy soil. *Environ. Microbiome* **2023**, *18*, 76. [[CrossRef](#)]
34. Anderson, C.R.; Peterson, M.E.; Frampton, R.A.; Bulman, S.R.; Keenan, S.; Curtin, D. Rapid increases in soil pH solubilise organic matter, dramatically increase denitrification potential and strongly stimulate microorganisms from the Firmicutes phylum. *PeerJ* **2018**, *6*, e6090. [[CrossRef](#)]
35. Ji, M.; Williams, T.J.; Montgomery, K.; Wong, H.L.; Zaugg, J.; Berengut, J.F.; Bissett, A.; Chuvochina, M.; Hugenholtz, P.; Ferrari, B.C. Candidatus Eremiobacterota, a metabolically and phylogenetically diverse terrestrial phylum with acid-tolerant adaptations. *ISME J.* **2021**, *15*, 2692–2707. [[CrossRef](#)] [[PubMed](#)]
36. Mao, Y.; Li, N.; Huang, Y.; Chen, D.; Sun, K. Divergence of rhizosphere microbial communities between females and males of the dioecious *Hippophae tibetana* at different habitats. *Microbiol. Spectr.* **2024**, *12*, e1624–e1670. [[CrossRef](#)]
37. Collingro, A.; Köstlbacher, S.; Horn, M. Chlamydiae in the Environment. *Trends Microbiol.* **2020**, *28*, 877–888. [[CrossRef](#)] [[PubMed](#)]
38. Garbeva, P.; Baggs, E.M.; Prosser, J.I. Phylogeny of nitrite reductase (nirK) and nitric oxide reductase (norB) genes from *Nitrospira* species isolated from soil. *FEMS Microbiol. Lett.* **2007**, *266*, 83–89. [[CrossRef](#)]
39. Yabe, S.; Sakai, Y.; Yokota, A. *Thermosporothrix narukonensis* sp. nov., belonging to the class Ktedonobacteria, isolated from fallen leaves on geothermal soil, and emended description of the genus *Thermosporothrix*. *Int. J. Syst. Evol. Microbiol.* **2016**, *66*, 2152–2157. [[CrossRef](#)]

40. Liang, F.; Huang, X.; Zheng, H.; Ma, X.; Huang, Y.; Sun, N.; Qin, X.; Jin, C.; Yu, L.; Cai, L. Characteristics of the soil bacterial community in the decomposition process inside and outside moso bamboo stumps. *Plant Soil* **2022**, *478*, 635–650. [[CrossRef](#)]
41. Fernández-González, A.J.; Villadas, P.J.; Díaz-Peña, F.; Notario-Del-Pino, J.; Lizano-Bastardín, Á.; Fernández-López, M.; León-Barrios, M. Key microorganisms defining the microbial communities of an alpine legume-shrubland ecosystem on a volcanic island in natural and fire-affected soils. *Plant Soil* **2024**, *498*, 651–670. [[CrossRef](#)]

**Disclaimer/Publisher’s Note:** The statements, opinions and data contained in all publications are solely those of the individual author(s) and contributor(s) and not of MDPI and/or the editor(s). MDPI and/or the editor(s) disclaim responsibility for any injury to people or property resulting from any ideas, methods, instructions or products referred to in the content.